

Pair-Breaking Edge of Superfluid $^3\text{He-B}$ in a Magnetic Field

R. Movshovich,^(a) N. Kim, and D. M. Lee

The Laboratory of Atomic and Solid State Physics and the Materials Science Center, Cornell University, Ithaca, New York 14853

(Received 18 September 1989)

We have conducted ultrasound pulse transmission experiments to investigate the pair-breaking edge for superfluid $^3\text{He-B}$ in a magnetic field. The experiments were performed at ^3He temperatures below $0.4T_c$, pressures between 6 and 29.3 bars, and ultrasound frequencies of 168.33, 137.6, and 107 MHz. We used both depressurization and demagnetization techniques to measure the linear and quadratic magnetic field dependence of the pair-breaking edge frequency. We obtain values for the Fermi-liquid interaction parameter F_2^q from the coefficient of the linear term. The quadratic term is due to the energy-gap distortion and its value is consistent with calculations of Schopohl and Tewordt.

PACS numbers: 67.50.Fi

The onset of superfluidity in ^3He is associated with the formation of an energy gap at the Fermi surface.¹ Proper analysis of such experimentally accessible quantities as collective-mode frequencies,² NMR shifts,^{1,2} and magnetic susceptibility³ requires an accurate determination of the magnitude of this gap. Recently, Adenwalla *et al.* have made zero-field pair-breaking measurements at high temperatures.⁴ In this paper we report on an experiment designed to use the pair-breaking frequency in $^3\text{He-B}$ as a direct measure of the superfluid energy gap in a magnetic field and at reduced temperatures $T/T_c < 0.45$.

We have performed high-frequency ultrasound pulse propagation experiments to probe the PB (pair-breaking) edge. The sound cell consisted of two matched quartz piezoelectric compressional transducers with a fundamental frequency of 15.2 MHz, separated by an optically flat spacer 4.5 mm long. The cell was mounted on a cryostat designed to operate at temperatures below 1 mK and in magnetic fields as high as 9 T.⁵ The temperature was measured by a ^3He -melting curve thermometer in a zero-field region linked to the ^3He of the sample cell by highly annealed silver rods. We derived our temperature scale from measurements of the melting pressure of ^3He by Osheroff and Yu,⁶ properly scaled to give the ordering temperature of solid ^3He on the melting curve as measured by Greywall.⁷

$^3\text{He-B}$ in zero magnetic field has an isotropic energy gap and is therefore an ideal candidate for investigation of the PB edge. At zero temperature and zero magnetic field the attenuation of zero sound of frequency ω associated with PB sets in when the energy of a phonon of that frequency becomes greater than twice the energy gap of the superfluid. The presence of a magnetic field has a twofold effect on the PB edge. The first is distortion of the energy gap itself.⁸ At low temperature this distortion results in a decrease in the longitudinal energy gap Δ_{\parallel} and an increase in the transverse energy gap Δ_{\perp} , corresponding to directions parallel and perpendicular to the applied field, respectively. The smaller longitudinal en-

ergy gap Δ_{\parallel} enters the expression for the PB edge, and can be expressed through the zero-field energy gap Δ_0 and effective Larmor frequency Ω_L as $\Delta_{\parallel}^2 = \Delta_0^2 - C\Omega_L^2$, where the coefficient C goes to $\frac{1}{2}$ as $T \rightarrow 0$.⁸ The second effect of the magnetic field is to introduce a Zeeman-like term linear in the magnetic field into the expression for the effective PB edge.⁹ This latter effect is associated with Zeeman splitting of the quasiparticle states. The final expression is found⁹ to be $\omega_{\text{PB}} = 2\Delta_{\parallel} - \Omega_L$, where the effective Larmor frequency is given by $\Omega_L = \Gamma H$ and

$$\Gamma = \frac{\gamma(1 + \frac{1}{5}F_2^q)}{1 + F_0^q[\frac{2}{3} + \frac{1}{3}Y(T)] + \frac{1}{5}F_2^q[\frac{1}{3} + (\frac{2}{3} + F_0^q)Y(T)]} \quad (1)$$

according to Sauls and Serene.¹⁰ Here F_0^q and F_2^q are the Fermi-liquid interaction parameters and $Y(T)$ is the Yosida function which goes from 0 at $T=0$ to 1 at T_c . The longitudinal energy gap can be expanded in magnetic field, and, keeping only the leading term in H^2 , we obtain $\Delta_{\parallel} = \Delta_0 - C\Omega_L^2/2\Delta_0$. The final expression for the effective pair-breaking frequency to second order in magnetic field becomes

$$\omega_{\text{PB}} = 2\Delta_0(P, T) - \Gamma(P, T)H - \frac{C\Gamma(P, T)^2}{\Delta_0(P, T)}H^2. \quad (2)$$

It is important to note that in many other experiments, such as measurement of the collective-mode frequencies using ultrasound, magnetic-susceptibility measurements, etc., it is difficult to separate the effects of F_2^q from the f -wave interaction parameter X_3 , both of which enter the appropriate expressions. On the other hand, the effective Larmor frequency is a function of F_2^q but does not depend on X_3 ,¹⁰ which makes an investigation of the PB edge of superfluid ^3He in a magnetic field perhaps a unique opportunity to study the parameter F_2^q independently from X_3 via the linear term in Eq. (2).

We can sweep the effective PB edge through the operating frequency of the sound transducers by sweeping temperature or pressure (thereby changing Δ_{\parallel}) or by

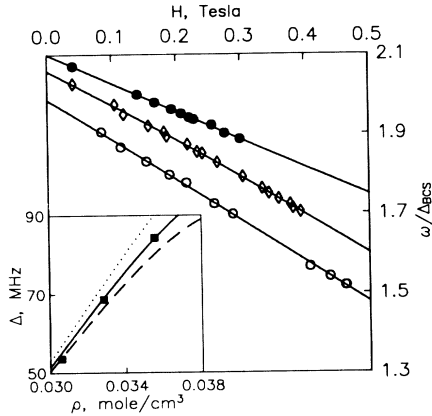


FIG. 1. Reduced effective PB edge as a function of magnetic field for three frequencies: ●, 168.33 MHz; ◇, 137.6 MHz, ○, 107 MHz. Inset: Measured energy gap vs ³He density. Lines are results of different theoretical calculations of energy gap: dotted, scaled Δ_{BCS}; solid, Δ₊; dashed, Δ_{BCS}.

sweeping magnetic field (and changing Ω_L). We operated the sound cell at frequencies of 168.33, 137.6, and 107 MHz, pressures between 6 and 29.3 bars, and magnetic fields up to 0.48 T. At the end of the PrNi₅ demagnetization the ³He sample temperature was around 550 μK. We then either swept the magnetic field at the rate of ≈0.01 T/hr or depressurized ³He at the rate of ≈0.01 bar/min to cross the PB edge. Sweeping the magnetic field generated the least amount of heating, and so most of the data were collected in that way. On several runs we collected data during the depressurization part of the cycle as well. During these runs depressurization would be stopped several times in the region of changing sound amplitude, allowing the system to come to equilibrium and the received pulses recorded.

We identified the PB edge by the position of the kink in the curves of received signal amplitude versus magnetic field or pressure. This kink was associated with the onset of attenuation of the sound pulse as we moved into the PB region by sweeping pressure or magnetic field. The uncertainty of the determination of the PB edge varied from 0.03% to 0.1% depending on the magnitude of the magnetic field and the method of crossing the PB

edge. Details of this part of the data reduction are given elsewhere.¹¹

We note here that the previously observed $J=1^-$ modes (of frequency 2Δ at zero field) couple to sound only for $H > 0$ and have a coefficient for Ω_L of $g=0.39$ as compared with unity for the PB edge.^{12,13} Therefore these modes fall above the PB edge and do not affect the position of the onset of attenuation.

Our data for all three frequencies are displayed in Fig. 1 as an effective PB frequency divided by the BCS energy gap versus magnetic field. The raw data have been corrected for temperature variation by normalizing points to a single temperature, which we chose to be zero. We did this by using the expression (1) for the effective Larmor frequency with the weak-coupling values of the Yosida function $Y(T)$ and Eq. (2) for the effective PB edge, where we have kept only the leading linear term in magnetic field. This procedure has an effect of shifting not only the temperature of the data points but pressure as well, since we are keeping the effective PB edge frequency constant. The amount of the shift in pressure was less than 1 bar for the data points taken at the highest temperature.

We fitted the data by a second-degree polynomial for each frequency. These fits are also plotted in Fig. 1. The zero-field extrapolations of the data give the pressure of superfluid ³He for the corresponding energy gaps, which are just half the sound frequencies. These values of pressure are given in Table I and also plotted in the inset of Fig. 1 together with three choices of the energy gap: the weak-coupling energy gap of BCS theory Δ_{BCS}, the result of the weak-coupling-plus theory of Serene and Rainer¹⁴ Δ₊, and the commonly used Δ_{BCS} energy gap scaled by the heat-capacity jump at the superfluid transition, Δ_{BCS}(δC/C_N)^{1/2}. The weak-coupling-plus energy gap fits the two higher-pressure experimental data points the best. The measured energy gap of the 4.85-bars point is depressed by 3% with respect to the weak-coupling-plus energy gap, which is outside the reputed uncertainty of the temperature scale, suggesting perhaps the need for negative correction to the temperature scale at low pressures or a revision of the theoretical prediction of the behavior of the energy gap of superfluid ³He-B at

TABLE I. Experimental values of the energy gap Δ_{expt} divided by the weak-coupling gap Δ_{BCS} and by the weak-coupling-plus (Ref. 14) gap Δ₊. Also shown are values of Γ and F₂^q calculated for different choices of the energy gap Δ₀ in Eq. (2). The lower bound Δ_{LB}, upper bound Δ_{UB}, and “best-guess” Δ_{BG} energy gaps for three pressure regions are chosen as described in the text and are also shown in Fig. 2. The value of C for the best-guess energy gap is also shown. Estimated errors in C are obtained from the variation in C corresponding to the above-mentioned choices of energy gap.

Pressure (bars)	$\frac{\Delta_{\text{expt}}}{\Delta_{\text{BCS}}}$	$\frac{\Delta_{\text{expt}}}{\Delta_+}$	Γ(Δ _{BG})	Γ(Δ _{LB})	Γ(Δ _{UB})	F ₂ ^q (Δ _{BG})	F ₂ ^q (Δ _{LB})	F ₂ ^q (Δ _{UB})	C
4.85	0.994	0.969	6.50 ± 0.03	6.25 ± 0.03	6.51 ± 0.03	0.45 ± 0.08	-0.14 ± 0.07	0.47 ± 0.08	0.43 ± 0.10
9.80	1.030	0.995	6.39 ± 0.03	6.13 ± 0.03	6.69 ± 0.04	-0.09 ± 0.07	-0.64 ± 0.07	0.64 ± 0.06	0.60 ± 0.10
18.10	1.050	1.002	6.45 ± 0.03	6.33 ± 0.03	6.674 ± 0.03	-0.19 ± 0.06	-0.46 ± 0.06	0.33 ± 0.07	0.54 ± 0.05

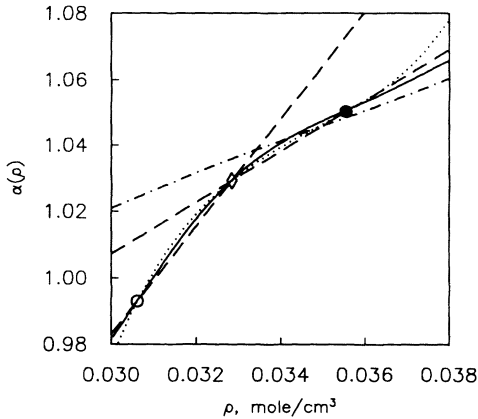


FIG. 2. The strong-coupling factor α vs ${}^3\text{He}$ density for the three zero-field data points (\bullet , 18.07 bars, 168.33 MHz; \diamond , 9.82 bars, 137.6 MHz; \circ , 4.85 bars, 107 MHz) with several fits as described in the text: dash-dotted, result of weak-coupling-plus theory (Ref. 14); dashed, straight lines through the neighboring points; dotted, quadratic fit of energy vs density; solid, best guess.

low pressures.

We have plotted the strong-coupling factor $\alpha(P, T) = \Delta_0(P, T)/\Delta_{\text{BCS}}(P, T)$ vs ${}^3\text{He}$ density in Fig. 2 for the three zero-field points obtained in the above analysis. Also plotted in Fig. 2 is the result of the weak-coupling-plus theory of Serene and Rainer,¹⁴ represented by the dash-dotted line. To obtain a "best guess" for the energy gap, plotted as a solid line, we first considered the straight line passing through the 9.82- and 18.07-bars data points as a lower bound, Δ_{LB} , between the two points and as an upper bound, Δ_{UB} , above 18.07 bars. Similarly, the straight line passing through the 4.85- and 9.82-bars points was used as a lower bound between them, and as a not very restrictive upper bound between 9.82 and 18.07 bars. For a lower bound at pressures above 18.07 bars we used the weak-coupling-plus energy gap, and for an upper bound between 4.85 and 9.82 bars we used a quadratic fit to the three data points (plotted as energy gap versus ${}^3\text{He}$ density as in the inset of Fig. 1). Our best guess was chosen to lie between the "limiting behaviors" and of course, pass through the data points, but is otherwise quite arbitrary.

In Fig. 3 we plot the data as $\omega_{\text{PB}}/\Delta_0(P, T=0)$ versus magnetic field, where we have used the best-guess energy gap Δ_{BG} from Fig. 2 to represent $\Delta_0(P, T=0)$. The data have been corrected for temperature variations as described above, and, through a similar procedure,¹¹ for the pressure variations within each set of data points at a particular frequency [via the dependence of Γ on $F_0^q(P)$]. The solid lines in Fig. 3 are quadratic fits to the data. To compare Eq. (2) with the experimental data, we divided it by $\Delta_0(P, T=0)$ and substituted the quadratic fits to the data for $\omega/\Delta_0(P, T=0)$ [and $1/\Delta_0(P, T=0)$]. Comparing the coefficients of like powers gave us the

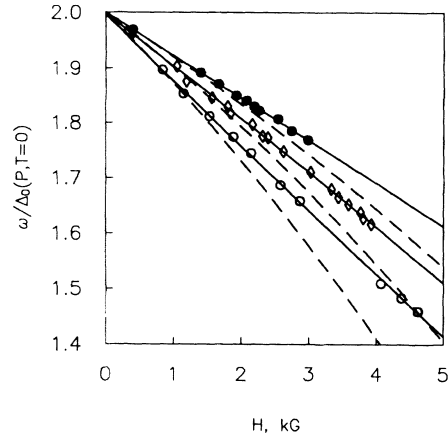


FIG. 3. $\omega/\Delta_0(P, T=0)$ vs magnetic field H for three PB frequencies: \bullet , 168.33 MHz; \diamond , 137.6 MHz; \circ , 107 MHz. The best-guess energy gap of Fig. 2 was used to represent $\Delta_0(P, T=0)$. The solid lines are quadratic fits to the data. The dashed lines are the constant-pressure curves for the effective PB edge for the three pressures of Table I, with the highest pressure at the top, which were obtained from Eq. (2) and best-guess values of F_0^q .

values of Γ and C . We used Γ to calculate the parameter F_0^q from the zero-temperature limit of the expression (1) for the effective Larmor frequency. Table I lists the values of Γ and F_0^q obtained for different choices for the energy gap Δ_0 that were shown in Fig. 2. We find that the values of the F_0^q parameter are small for the range of pressures studied in this experiment, and that they are rather sensitive to the zero-field energy gap as a function of pressure. To avoid this complication and simplify our analysis we are preparing a similar experiment with a cell containing broadband sound transducers with the capability to sweep sound frequency for a variety of magnetic field values at a constant pressure of ${}^3\text{He}$. Also shown in Table I are the values for the coefficient C of the quadratic term that is a result of the energy-gap distortion and which is predicted to go to $C = \frac{1}{2}$ as $T \rightarrow 0$ by Tewordt and Schopohl.⁸ Our results are in good agreement with their prediction. We used the values for Γ and C from Table I to calculate the effective PB edge as a function of the magnetic field for the three pressures of Table I. The resulting *constant-pressure* rather than constant-PB-frequency curves are plotted in Fig. 3 as dashed lines. Here the effect of the nonlinear term is much more pronounced since it is no longer masked by the pressure variation. The linear term, however, has a significantly larger effect than the quadratic term.

In conclusion, we have used ultrasound pulse propagation to measure the PB edge frequency as a function of magnetic field for three different frequencies. The magnetic field has a very strong effect on the pair-breaking edge, reducing it substantially. We have measured both linear and quadratic terms in the field dependence, corre-

sponding to the effects of quasiparticle Zeeman splitting and gap distortion, respectively, as well as the zero-field energy gap in the low-temperature regime. The zero-field energy gap very closely follows the weak-coupling-plus¹⁴ energy gap in the intermediate- and high-pressure regimes but deviates from it in the low-pressure regime. Over the pressure range studied, we obtained values for the elusive F_2^q parameter which cluster around zero. Our results fall between the F_2^q values deduced¹⁵ from the real-squashing-mode field splitting,¹⁶ and the values based¹³ on magnetic-susceptibility measurements.¹⁷ They are also in substantial disagreement with recent longitudinal magnetic resonance data.¹⁸ The coefficient of the quadratic term agrees well with the theoretical prediction of Tewordt and Schopohl.⁸

We wish to thank the National Science Foundation for supporting this research via Grant No. DMR-841605 and through the Cornell Materials Science Center via Grant No. DMR-8516616. One of us (R.M.) would like to thank AT&T Bell Laboratories for support and another of us (D.M.L.) wishes to acknowledge the hospitality of the Aspen Center for Physics. We are grateful to Mark Meisel for providing us with his version of Peter Wölfle's programs as well as a store of other information, and to Eric Varoquaux, Wojciech Wojtanowski, Ross McKenzie, Jim Sauls, and Daryl Hess for stimulating and informative discussions. We are especially grateful to Joe Serene for his highly constructive criticism and generous help. Finally, we thank David Sagan, Larry Friedman, Emil Polturak, Paul de Vegvar, and Eric Ziercher for designing and constructing some of the apparatus used in these experiments.

^(a)Current address: AT&T Bell Laboratories, Murray Hill, NJ 07974.

¹A. J. Leggett, *Rev. Mod. Phys.* **47**, 331 (1975).

²P. Wölfle, *Physica (Amsterdam)* **90B+C**, 96 (1977); D. M. Lee and R. C. Richardson, in *The Physics of Liquid and Solid Helium, Part II*, edited by K. H. Benneman and J. B. Ketterson (Wiley, New York, 1978), pp. 287-496.

³N. Schopohl, *J. Low Temp. Phys.* **49**, 347 (1982).

⁴S. Adenwalla, Z. Zhao, J. B. Ketterson, and Bhimal K. Sarma, *Phys. Rev. Lett.* **63**, 1811 (1989).

⁵D. C. Sagan, Ph.D. thesis, Cornell University, 1984 (unpublished).

⁶D. D. Osheroff and C. Yu, *Phys. Lett.* **77A**, 458 (1980).

⁷D. S. Greywall, *Phys. Rev. B* **33**, 7520 (1986).

⁸L. Tewordt and N. Schopohl, *J. Low Temp. Phys.* **37**, 421 (1979); N. Schopohl, M. Warnke, and L. Tewordt, *Phys. Rev. Lett.* **50**, 1066 (1983).

⁹N. Schopohl and L. Tewordt, *J. Low Temp. Phys.* **57**, 601 (1984).

¹⁰J. A. Sauls and J. W. Serene, *Phys. Rev. Lett.* **49**, 1183 (1982).

¹¹R. Movshovich, Ph.D. thesis, Cornell University, 1990 (unpublished); (to be published).

¹²E. R. Dobbs, R. Ling, and J. Saunders, in *Proceedings of the Seventeenth International Conference on Low Temperature Physics*, edited by U. Eckern, A. Schmid, W. Weber, and H. Wuhl (North-Holland, Amsterdam, 1984), p. 763.

¹³N. Schopohl and L. Tewordt, in *Proceedings of the Seventeenth International Conference on Low Temperature Physics*, edited by U. Eckern, A. Schmid, W. Weber, and H. Wuhl (North-Holland, Amsterdam, 1984), p. 777.

¹⁴J. W. Serene and D. Rainer, *Phys. Rep.* **101**, 221 (1983).

¹⁵R. S. Fishman and J. A. Sauls, *Phys. Rev. B* **38**, 2526 (1988).

¹⁶O. Avenel, E. Varoquaux, and H. Ebisawa, *Phys. Rev. Lett.* **45**, 1952 (1980).

¹⁷H. N. Scholz, Ph.D. thesis, Ohio State University, 1981 (unpublished); R. F. Hoyt, H. N. Scholtz, and D. O. Edwards, *Physica (Amsterdam)* **107B**, 287 (1981).

¹⁸D. Candela, D. O. Edwards, A. Heff, N. Masuhara, Y. Oda, and D. S. Sherrill, *Phys. Rev. Lett.* **61**, 420 (1988).